



Research article

Inclusions of diamond crystals in the tourmaline of the schorl-uvite series: problems of genesis

Andrei V. KORSAKOV¹✉, Denis S. MIKHAILENKO¹, LE ZHANG², YI-GANG XU²¹ V.S.Sobolev Institute of Geology and Mineralogy Siberian Branch RAS, Novosibirsk, Russia² State Key Laboratory of Isotope Geochemistry and CAS Center for Excellence in Deep Earth Science, Guangzhou Institute of Geochemistry, Chinese Academy of Science, Guangzhou, China

How to cite this article: Korsakov A.V., Mikhailenko D.S., Zhang Le., Xu Yi-Gang. Inclusions of diamond crystals in the tourmaline of the schorl-uvite series: problems of genesis. *Journal of Mining Institute*. 2023. Vol. 264, p. 833-841. EDN UMQOXX

Abstract. The mineralogical and geochemical features of diamond-bearing tourmaline crystals (schorl-uvite series) from garnet-clinopyroxene rocks of the Kumdy-Kol deposit (Northern Kazakhstan) have been studied in detail. The formation of the main rock-forming minerals (garnet + K-bearing clinopyroxene) occurred in the diamond stability field at 4-6 GPa and 950-1000 °C. Crystallization of K-bearing clinopyroxene at these parameters is possible in the presence of an ultra-potassic fluid or melt formed because of crustal material melting in subduction zones. Tourmaline crystals (up to 1 cm) containing diamond inclusions perform veins crosscutting high-pressure associations. The composition of individual zones varies from schorl to uvite within both a single grain and the sample as a whole. The potassium content in this tourmaline does not exceed 0.1 wt.% K₂O, and the isotopic composition of boron $\delta^{11}\text{B}$ varies from -10 to -15.5 ‰, which significantly differs from the previously established isotopic composition of boron in maruyamaite crystals ($\delta^{11}\text{B}$ 7.7 ‰ in the core and -1.2 ‰ in the rim) of the same deposit. Analysis of the obtained data on $\delta^{11}\text{B}$ in the tourmalines from the diamond-grade metamorphic rocks within the Kumdy-Kol deposit suggests the existence of two boron sources that resulted in crystallization of K-bearing tourmaline crystals (maruyamaite-dravite series) and potassium-free tourmalines of the schorl-uvite series.

Keywords: tourmaline; diamond; boron isotopic composition; silicate-carbonate rocks; subduction; high pressure metamorphism; Kokchetav

Acknowledgment. The study was financially supported by RSF N 18-17-00186.

Received: 01.12.2022

Accepted: 19.01.2023

Online: 18.05.2023

Published: 25.12.2023

Introduction. Accessory minerals (zircon [1-3], cassiterite [4], beryl [5, 6], etc.) and the peculiarities of their composition are widely used in modern mineralogical and petrological reconstructions. Tourmaline is one of such unique minerals, stable in a wide range of temperatures and pressures [7, 8], that allows to reconstruct the composition of the fluid phase in the subduction zones [9, 10]. Tourmaline has proven to be a reliable tool in the investigation of the evolution of the fluid composition in diverse mineral deposits [11, 12]. The identification of diamond crystal inclusions within potassium-rich tourmaline crystals [13] in the rocks of the Kumdy-Kol industrial diamond deposit in the Kokchetav massif of Northern Kazakhstan has yielded valuable scientific insights. This discovery suggests that the crystallization of the tourmaline began at the peak of metamorphism, occurring at 6 GPa and approximately at 1000 °C, within the diamond stability field. Moreover, this finding has led to the recognition of a new tourmaline end-member maruyamaite [14]. However, Ar-Ar dating of K-bearing tourmaline [15] and the absence of other high-pressure mineral inclusions in this mineral [7, 16] led to doubt the high-pressure origin of maruyamaite. The successful synthesis of K-dravite was carried out at a pressure of 4 GPa and 700 °C from an ultra-potassic fluid [17-19], which renewed



interest in the high-pressure model of maruyamaite formation. Earlier, another K-containing mineral, clinopyroxene (with a K_2O content of up to 1.5 wt.%), was identified in the rocks of the Kokchetav massif. The origin of this mineral is also associated with high pressures and temperatures in the presence of an ultra-potassic fluid (melt) [20-22]. Traces of the existence of ultra-potassium fluids (melts) in the same rocks were identified in submicron-sized inclusions in diamond crystals [23], as well in rock-forming minerals [24]. Inclusions of diamond crystals in tourmaline were first found in the same rock type by V.S.Shatsky, but the composition of tourmaline is unknown. Unlike kimberlite diamond crystals, the high-pressure origin of which is beyond doubt [25], the first finds of diamond crystals in low-pressure minerals led to the appearance of a metastable model of diamond formation in crustal metamorphic rocks [26]. This article presents the results of an isotope-geochemical study of crystals of diamond-bearing tourmaline from garnet-clinopyroxene rocks of the Kumdy-Kol deposit, and enhances our understanding of the behavior of boron-bearing fluids and melts and of their mobility in subduction zones.

The Kokchetav massif has become widely known due to discovery of diamond in the crustal metamorphic rocks [27]. It is located in the central part of the Ural-Mongolian folded belt [28]. The Kokchetav massif considered to be a megamelange zone more than 80 km long and about 17 km wide [28]. Kumdy-Kol is the most famous site of ultrahigh-pressure rocks within the Kokchetav massif. Kumdy-Kol microdiamonds deposit is located on the southern shore of the lake of the same name. The internal structure of this block has been ascertained through the results of meticulous geological exploration efforts performed in the process of evaluating the reserves of the deposit. Structurally, the rocks of the Kumdy-Kol block are oriented subvertically with steeply dipping beds ($\sim 70^\circ$) in the southwest direction. The following rocks types are recognized here: eclogites, amphibolites, carbonate-silicate rocks, migmatites, shales, and various gneisses, which are the main type of ores [26, 27, 29]. A detailed description of the rocks and ores of the Kumdy-Kol deposit can be found in publications [30, 31].

Methods. All analyses were obtained at the Analytical Center for multi-elemental and isotope research SB RAS and the Institute of Geochemistry CAN (Guangzhou, China). The composition of minerals was determined using a Jeol JXA-8100 microprobe with an accelerating voltage of 20 kV and a probe current of 30 nA. Natural minerals and synthetic analogues were used as standards [32].

In situ analyses of the isotopic composition of boron in tourmaline was carried out on Neptune Plus MC-ICP-MS and ELEMENT XR (Thermo Fisher Scientific) equipped with a laser ablation system (ArF) with a 193 nm laser (Resolution M-50, Resonetics LLC, USA) at the Institute of Geochemistry, CAN. IMR RB2 -12.53 ± 0.57 % was used as the standard for determining the isotopic composition of boron; when determining the concentration of trace elements, calibration was performed on TB-1G, BCR-2G, BHVO-2G and GSD-1G with further normalization for the SiO_2 content in tourmaline. This technique is described in detail in [33]. The abbreviation of minerals is given according to the publication [34].

Results and discussion. A sample of garnet-clinopyroxene rock (O24-16) was collected in the gallery (24 ort) of the Kumdy-Kol microdiamond deposit. These rocks consist of garnet (60 vol.%) and K-bearing clinopyroxene (40 vol.%). In interstitials between garnet and clinopyroxene porphyroblasts, potassium feldspar (Kfs) and, less frequently, calcite are present in insignificant amounts. In the studied sample, the interlayers enriched with garnet and clinopyroxene are folded (Fig.1). Tourmaline occupies the central parts of the crosscutting veins, the thickness of which can reach 1.5 cm (Fig.1, a). Chlorite and amphibole zones are observed around these veins (Fig.1, b).

Diamond, rutile, clinopyroxene occur as inclusions in the garnet (Fig.2). Clinopyroxene contains inclusions of diamond, garnet and rutile in the cores along with the exsolution lamellae of Kfs and phengite (Fig.3, a, b). Inclusions of diamond crystals occur in tourmaline crystals (Fig.3, c, d), as well as in amphibole-chlorite aggregates replacing garnet and clinopyroxene. The morphology of all diamond crystals are independent of the host mineral.

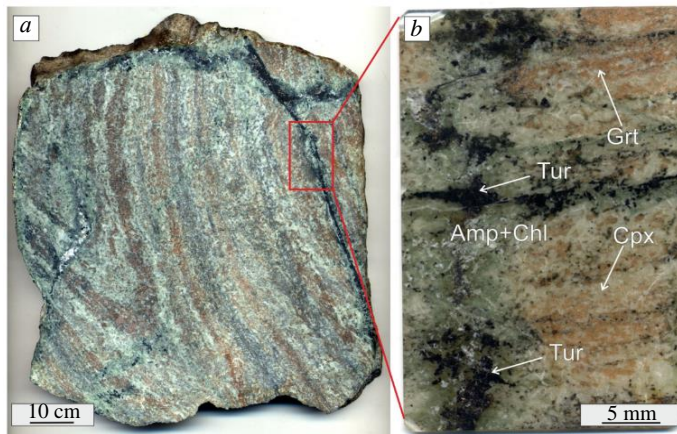


Fig.1. Tourmaline-bearing garnet-clinopyroxene rock from the exploration gallery of the Kumdy-Kol deposit diamonds (24 ort): *a* – sample section; *b* – micrograph of the polished plate of the sample fragment, demonstrating the substitution of primary associations with amphibole and chloride along the tourmaline veins

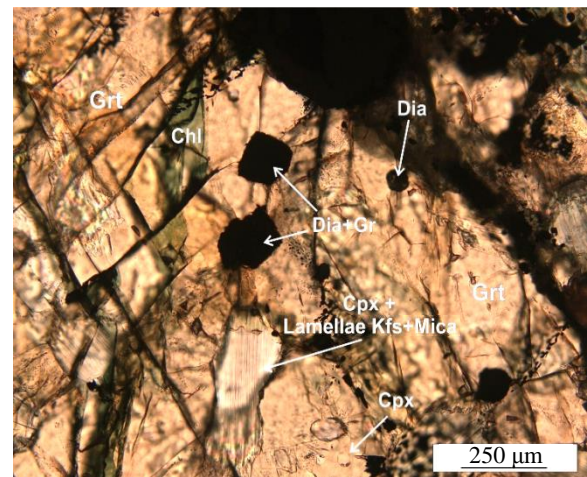


Fig.2. Micrograph of a polished plate of a fragment of a garnet-clinopyroxene rock sample, demonstrating a variety of mineral inclusions in garnet porphyroblasts

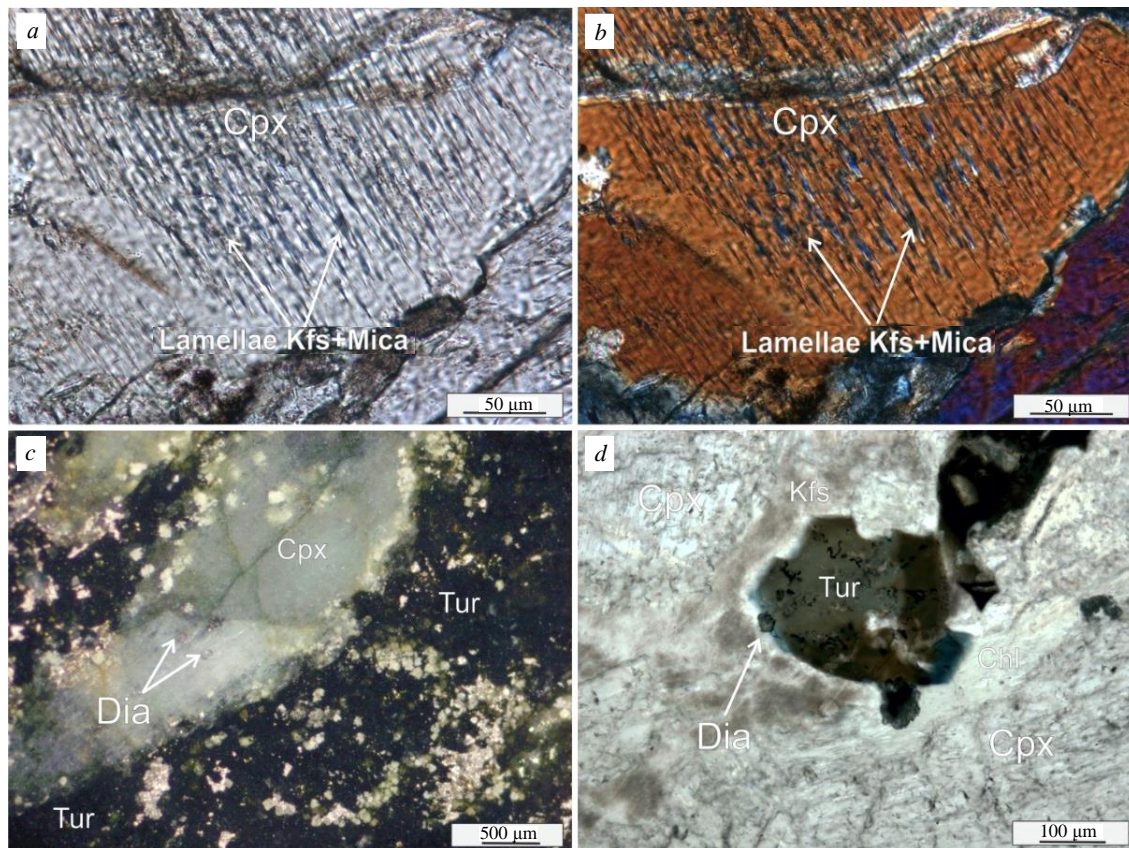


Fig.3. Micrographs of individual sections of the sample of the garnet-clinopyroxene rocks (sample O24-16): *a, b* – clinopyroxene porphyroblasts with exsolution lamellae in the core, surrounded by a clean rim (nichols are parallel and crossed, respectively); *c* – numerous inclusions of diamond crystals (pale yellow crystals) in clinopyroxene and tourmaline; *d* – inclusions of diamond crystals in various zones of tourmaline grains

The compositions of garnet and clinopyroxene crystals are identical to the compositions of the garnet and clinopyroxene of the previously studied samples of garnet-clinopyroxene rocks from the Kokchetav massif [27, 29]. Garnet porphyroblasts are solid solutions of the pyrope-grossular-almandine, with a homogeneous core ($\text{Alm}_{23}\text{Sp}_{82}\text{Prp}_{25}\text{Grs}_{50}$), and the main compositional changes occur



Analysis of tourmaline from a sample of garnet-clinopyroxene rocks (sample O24-16)

Composition		Crystal zone	
		Core	Rim
SiO ₂		35.8	36.0
TiO ₂		0.51	0.65
Al ₂ O ₃		30.0	29.6
Cr ₂ O ₃		bdl	bdl
FeO		10.80	6.48
MnO		0.07	0.08
MgO		6.1	9.2
CaO		2.16	3.16
Na ₂ O		1.67	1.25
K ₂ O		0.09	0.05
F		n.a.	n.a.
Σ		87.2	86.5
B	B	3.00	3.00
T	Si	5.98	5.97
	Al	0.02	0.03
	Σ	6.00	6.00
Al (total)		5.92	5.78
Z	Al	5.90	5.75
	Cr	0.00	0.00
	Mg	0.10	0.25
	Σ	6.00	6.00
Y	Al	0.00	0.00
	Ti	0.06	0.08
	Cr	0.00	0.00
	Fe ²⁺	1.51	0.90
	Mn ²⁺	0.01	0.01
	Mg	1.41	2.01
Σ	3.00	3.00	
X	Ca	0.39	0.56
	Na	0.54	0.40
	K	0.02	0.01
	Vacancy	0.05	0.03
	Σ	1.00	1.00
OH (V+W)		3.66	3.59
V	OH	3.00	3.00
	O	0.00	0.00
W	OH	0.66	0.59
	F	0.00	0.00
	O	0.34	0.41
V+W total		4.00	4.00

Notes: bdl – below the limits of detection; n.a. – was not analyzed. Structural formula of tourmaline $XY_3Z_6(T)_6(B)_3O_{18}V_3W$, where X = (Na, Ca, vacancy); Y = (Fe^{2+/3+}, Mg, Mn, Al, Li, Cr, V); Z = (Mg, Fe³⁺, Al, Cr, V); T = (Si, Al); B = (BO₃); V = (OH, O); W = (OH, F, O).

tourmaline grains of the schorl-uvite series, since the stability field for tourmaline of this composition has not been studied experimentally. Experimental studies of the stability field of dravite in the metapelite system reveal that this phase remains stable up to pressures of 5 GPa at ~700 °C [37]. However, the schorl is less stable and its decomposition starts at a pressure of 3.5 GPa [38]. At ambient pressure the breakdown of uvite occurs in the temperature range of 800-900 °C [39], and the products are the rare mineral assemblage indialite (Mg₂Al₄Si₅O₁₈) + yuanfuliite (Mg_{0.75}Fe²⁺_{0.3}Fe³⁺_{0.5}Al_{0.2}Mg_{0.1}Ti_{0.1}(BO₃)O) + plagioclase + boron-bearing mullite + hematite. The

within the thin rims. In the rim zones, the grossular content increases while the pyrope content (Alm₂₃Sps₂Prp₂₁Gr₅₄) decreases simultaneously. The content of almandine and spessartine remains almost constant. Clinopyroxene porphyroblasts have diopside – hedenbergite compositions. In clinopyroxene porphyroblast cores K₂O content does not exceed 0.3 wt.%, however, the presence of numerous exsolution lamellae Kfs and micas (Fig.3, a, b) identified by microprobe analysis (Fig.3, a, b) indicates that it was originally potassium-rich clinopyroxene. There are no exsolution lamellae in the rim zones of porphyroblasts, and the K₂O content is below the detection limit.

Macroscopically, in the studied sample tourmaline crystals look almost black (Fig.3, c), whereas in the thin sections they are characterized by a pronounced color zonation – a brown core and a blue rim (Fig.3, d). According to the chemical composition, these zones can be assigned to schorl and uvite according to the classification [35], where the formula coefficients were calculated in accordance with the recommendations [35] (see Table, Fig.4).

Inclusions of diamond crystals (10-300 microns in size) were identified in all zones of tourmaline crystals (see Fig.3, c, d). This is the first finding of diamond of inclusions in tourmalines of the schorl-uvite series. Previously, diamond inclusions were found exclusively in maruyamaite crystals [13] and were used as one of the proofs of the high-pressure origin of this unusual tourmaline. The abnormally high potassium contents and unusual isotopic boron composition in maruyamaite were also considered an evidence of the high-pressure formation of this mineral [13, 36]. In the studied sample, tourmaline veins crosscut the initially high-pressure minerals – garnet and K-bearing clinopyroxene (see Fig.1) and unequivocally prove that the process of tourmaline crystallization is temporally distinct from the formation of the primary rock-forming mineral assemblage. Very low potassium concentrations in the studied tourmaline (see Table) do not allow one to date the time of its formation by the Ar-Ar method [15] and indicate that the ultra-potassic liquid, which is the crystallization medium for K-bearing clinopyroxene, could not be the same for tourmaline. It appears impossible to get reliable estimates of the physico-chemical conditions of crystallization of

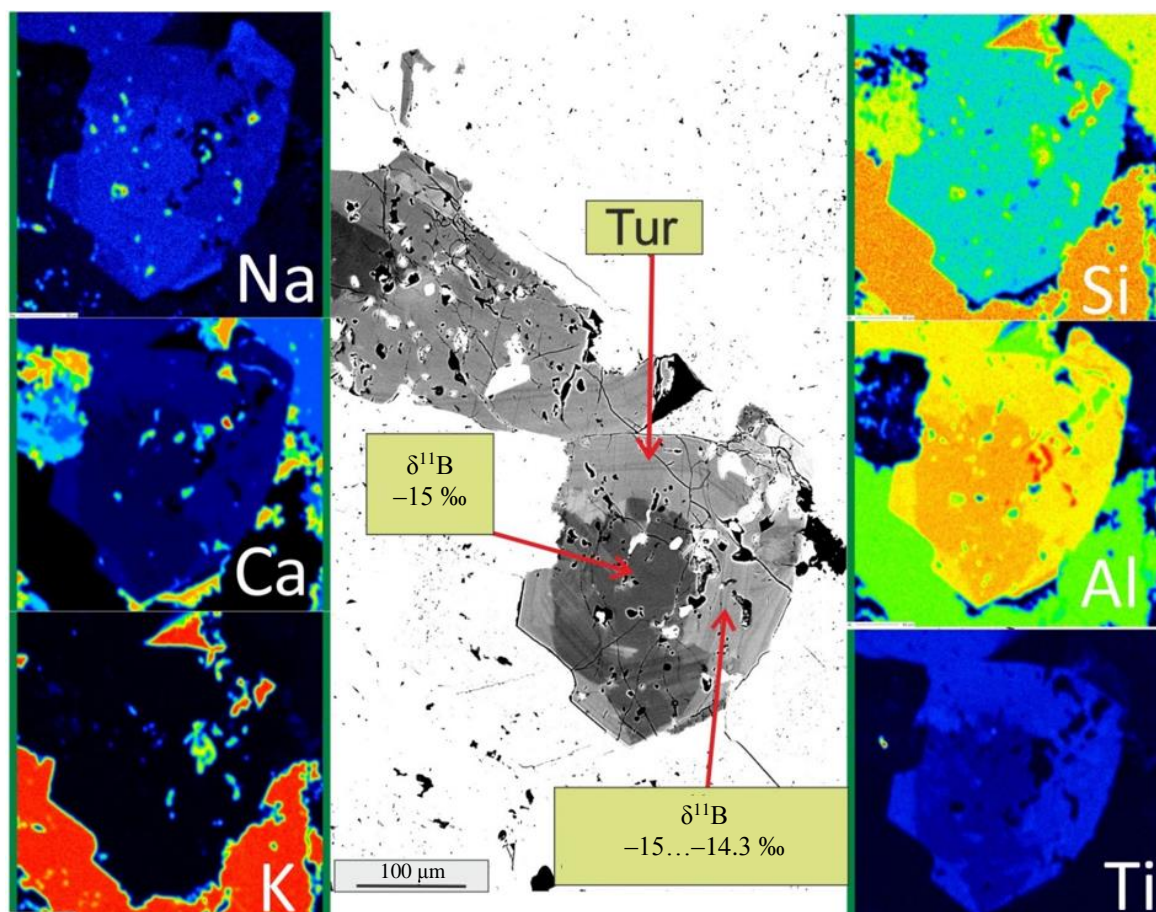


Fig.4. Backscattered electron image and characteristic X-ray maps of element distribution of the tourmaline crystal (see Fig.3, *d*)

effect of pressure on the stability of this type of tourmaline has not yet been investigated. Taking into account these experimental data, it can be assumed that the crystallization of the tourmaline of the schorl-uvite series should occur at a retrograde stage at a pressure below 3.5 GPa and temperature < 900 °C. The coexistence of tourmaline with Kfs (Fig.3, *d*) further reduces the pressure range in which joint crystallization of these minerals can occur, since Kfs is unstable in a water-bearing system at pressures above 2 GPa and 600 °C [40], whereas in a dry system tourmaline has not been synthesized [41]. The presence of chlorite- and amphibole-rich zones around tourmaline veins (see Fig.1, *b*) indicates that tourmaline crystallization likely took place before the formation of the mineral assemblages typical of the greenschist metamorphic facies.

The analysis of the boron isotopic composition $\delta^{11}\text{B}$ in tourmaline crystals of the schorl-uvite series varies from -10 to -15.5 ‰ and differs significantly from the isotopic composition of maruyamaite crystals ($\delta^{11}\text{B}$ 7.7 ‰ in the core and -1.2 ‰ in the rim) [7, 36]. There are two alternative models to explain the unusual isotopic composition of boron in maruyamaite crystals [7, 36]. According to the model proposed in [36], the boron isotopic composition is associated with the subduction of crustal material to depths of more than 120 km and with the crystallization of maruyamaite near the peak of metamorphism from the fluids derived during the dehydration of serpentinized rocks of the lithospheric mantle. However, within the Kokchetav massif, ultramafic rocks are extremely rare and within the western Kundy-Kol block, there is only a small outcrop of garnet-clinohumite rocks [42]. An alternative model [7] suggests that this isotopic composition of boron in maruyamaite could have arisen because of chromatographic effect during infiltration of boron-rich fluid in mid-crustal conditions. High content of tourmaline (up to 30 vol.%) in these rocks excludes the possibility of its formation due to boron present in the protolith. Thus, the formation of tourmaline-rich rocks of the maruyamaite-dravite series is possible with an intensive metasomatic transformation of the original substrate. Ar-Ar



dating of potassium-bearing tourmaline crystals has revealed a significant temporal discontinuity between its crystallization and the formation of high-pressure mineral assemblages [15]. The obtained isotopic data (Fig.5) are characteristic of the tourmaline crystals, the formation of which is associated with the fractionation of the boron isotopic composition resulting from metamorphic reactions of mica dehydration. The isotopic characteristics of the tourmaline crystals are similar to those found in rocks of the continental crust. [7, 36]. The formation of tourmaline veins also requires a significant input of boron [7, 43], since its content in meta-sediments rarely exceeds 50-150 ppm [44]. In high-pressure metamorphic rocks the formation of a boron-enriched fluid is usually associated with the decomposition of muscovite-phengite mica at the progressive stage of metamorphism during the subduction of crustal rocks [45]. However, according to experimental data [40], phengite can be stable in rocks of the Kokchetav massif up to the peak of metamorphism, and its decomposition may begin at the initial stages of exhumation with the formation of a melt [46]. These high-pressure melts can

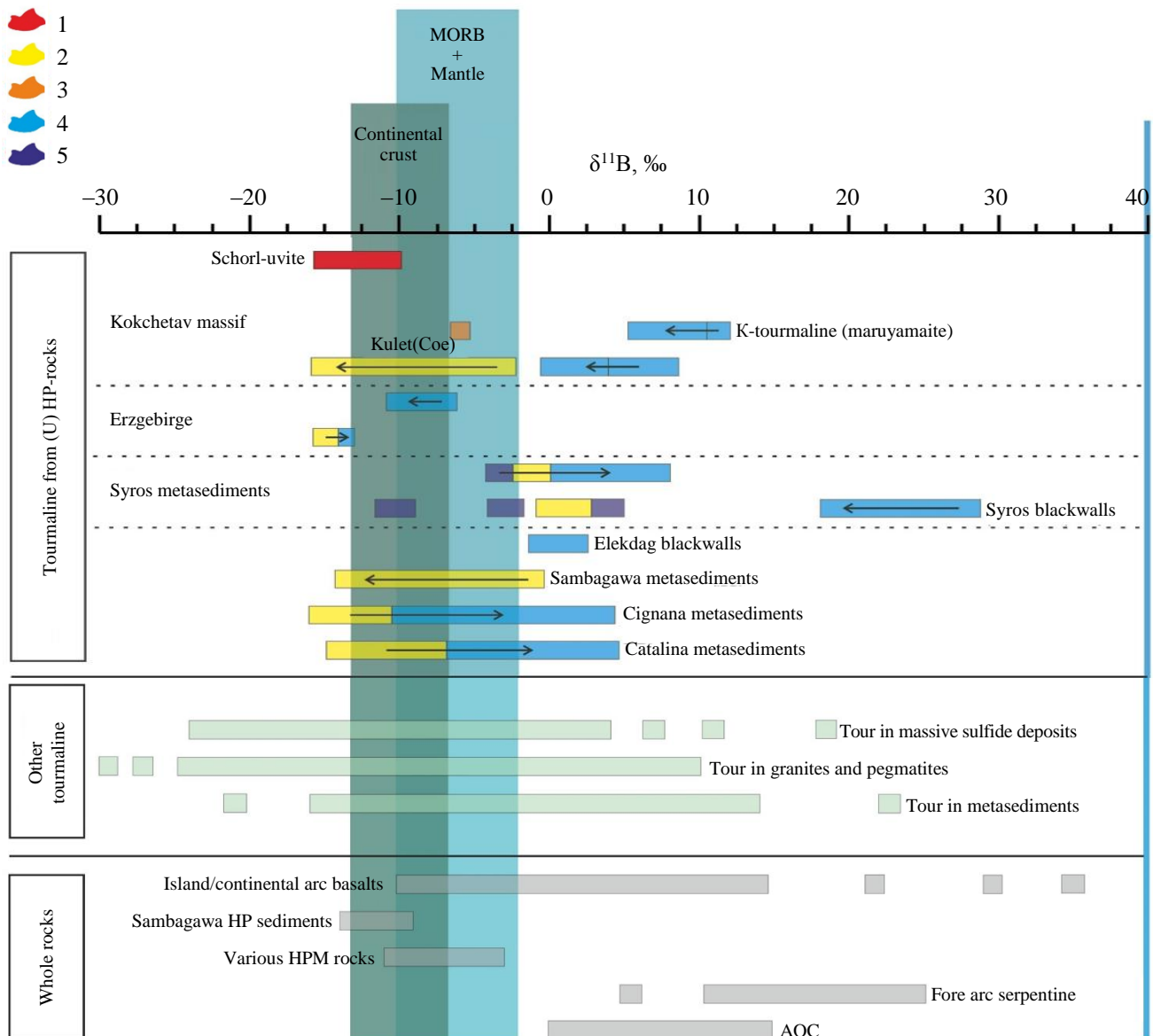


Fig.5. Boron isotopic composition in schorl-uivite series tourmaline crystals (red rectangle) from diamond-bearing rocks of the Kokchetav massif in comparison with the compositions of tourmaline from other types of rocks and some of the most important geochemical reservoirs [7] (arrows show the change in the composition of boron in zonal tourmaline grains and are directed from the core to the rim)

1 – authors' data; 2-5 – types: 2 – A1 (boron released from mica); 3 – A2 (decomposition of boron-bearing minerals); 4 – B (metasomatic influx of boron); 5 – C (detrital cores); MORB – basalts of mid-oceanic ridges; HP-sediments – metamorphosed sediments under high-pressure conditions; HPM-rocks – high-pressure metamorphic rocks



harbor a considerable quantity of water (up to 30 wt.%) and other elements, among them boron. The separation of the fluid from this melt is likely to occur at relatively shallow depths (40 km), which may indirectly provide evidence in favor of the formation of tourmaline in the final stages of exhumation of high-pressure rocks. Earlier studies have suggested the formation of certain tourmaline crystals during the regressive stage [13]. However, due to the absence of isotopic data, the sources and timing of boron-bearing fluids involved in the process were not addressed. The discovery of diamond-bearing tourmaline crystals (of the maruyamaite-dravite and schorl-uvite series) that exhibit distinct isotopic and compositional characteristics suggests that the formation of tourmaline at the Kumdy-Kol deposit was not due to a single large source of boron-bearing fluid. Most likely, the mobility of boron-bearing fluids was limited during the crystallization of various varieties of tourmaline, regardless of the conditions (pressure and temperature) of their formation. Furthermore, beyond the boron isotopic composition, the composition of these fluids may exhibit variations in terms of their potassium content. This can be attributed to the fact that the successful synthesis of potassium-bearing tourmaline (maruyamaite-dravite series) is exclusively observed in the presence of ultra-potassic fluid [17, 18]. Relics of ultra-potassic fluids were detected in submicron-sized inclusions in diamond crystals that came from metamorphic rocks of the Kokchetav massif [23]. However, due to the small size of the inclusions, boron concentration was not measured. In rock-forming minerals of garnet-clinopyroxene rocks, products of the crystallization of high-pressure melts [24] were identified in garnet and clinopyroxene. These inclusions have high potassium contents; the boron concentrations are as high as 28 ppm [24]. Fractionation and evolution of the composition of these melts during the retrograde stage of metamorphism could lead to the separation of fluids enriched in boron and potassium. These fluids are a prerequisite for the crystallization of potassium-bearing tourmaline of the maruyamaite-dravite series, and one should expect to find them in garnet-clinopyroxene rocks. In contrast, only schorl-uvite series tourmaline crystals with a potassium concentration of up to 0.1 wt.% (see Table) containing diamond inclusions were found (see Fig.3) in garnet-clinopyroxene rocks. This finding excludes the possibility of the participation of high-pressure fluids and (or) melts in the formation of diamond-bearing tourmaline crystals in the studied samples. Diamond crystals are relics of the ultra-high pressure mineral assemblage destroyed to varying degrees by later metasomatic processes in garnet-clinopyroxene and tourmaline-Kfs-quartz rocks of the Kumdy-Kol deposit.

Conclusions. The comprehensive mineralogical and geochemical study of diamond-bearing tourmaline crystals (schorl-uvite series) from garnet-clinopyroxene rocks of the Kumdy-Kol deposit (Northern Kazakhstan) and comparison with previously published data for maruyamaites have revealed the existence of contrasting sources of boron-bearing fluid (enriched in heavy and light boron isotopes) that led to the formation of the mentioned tourmaline varieties within one deposit. If the formation of tourmalines occurred synchronously, then the mobility of fluids in deeply subducted crustal rocks was very limited. The identification of diamonds in mineral inclusions should be approached with great prudence when it comes to subsequent petrological reconstructions, owing to the notable resistance of this mineral to retrograde transformations of mineral assemblages in high-pressure rocks.

REFERENCES

1. Melnik A.E., Korolev N.M., Skublov S.G. et al. Zircon in mantle eclogite xenoliths: a review. *Geological Magazine*. 2021. Vol. 158. Iss. 8, p. 1371-1382. DOI: [10.1017/S0016756820001387](https://doi.org/10.1017/S0016756820001387)
2. Skublov S.G., Rummyantseva N.A., Qiuli Li et al. Zircon Xenocrysts from the Shaka Ridge Record Ancient Continental Crust: New U-Pb Geochronological and Oxygen Isotopic Data. *Journal of Earth Science*. 2022. Vol. 33. Iss. 1, p. 5-16. DOI: [10.1007/s12583-021-1422-2](https://doi.org/10.1007/s12583-021-1422-2)
3. Skublov S.G., Makeev A.B., Krasotkina A.O. et al. Isotopic and Geochemical Features of Zircon from the Pizhemskeye Titanium Deposit (Middle Timan) as a Reflection of Hydrothermal Processes. *Geokhimiya*. 2022. Vol. 67. N 9, p. 807-829 (in Russian). DOI: [10.31857/S0016752522090060](https://doi.org/10.31857/S0016752522090060)
4. Rizvanova N.G., Alenicheva A.A., Skublov S.G. et al. Early Ordovician Age of Fluorite-Rare-Metal Deposits at the Voznesensky Ore District (Far East, Russia): Evidence from Zircon and Cassiterite U-Pb and Fluorite Sm-Nd Dating Results. *Minerals*. 2021. Vol. 11. Iss. 11. N 1154. DOI: [10.3390/min11111154](https://doi.org/10.3390/min11111154)



5. Skublov S.G., Gavrilchik A.K., Berezin A.V. Geochemistry of beryl varieties: comparative analysis and visualization of analytical data by principal component analysis (PCA) and t-distributed stochastic neighbor embedding (t-SNE). *Journal of Mining Institute*. 2022. Vol. 255, p. 455-469. DOI: [10.31897/PMI.2022.40](https://doi.org/10.31897/PMI.2022.40)
6. Abdel Gawad A.E., Ene A., Skublov S.G. et al. Trace Element Geochemistry and Genesis of Beryl from Wadi Nugrus, South Eastern Desert, Egypt. *Minerals*. 2022. Vol. 12. Iss. 2. N 206. DOI: [10.3390/min12020206](https://doi.org/10.3390/min12020206)
7. Marschall H.R., Korsakov A.V., Luvizotto G.L. et al. On the occurrence and boron isotopic composition of tourmaline in (ultra) high-pressure metamorphic rocks. *Journal of the Geological Society*. 2009. Vol. 166. Iss. 4, p. 811-823. DOI: [10.1144/0016-76492008-042](https://doi.org/10.1144/0016-76492008-042)
8. Berryman E.J., Dongzhou Zhang, Wunder B., Duffy T.S. Compressibility of synthetic Mg-Al tourmalines to 60 GPa. *American Mineralogist*. 2019. Vol. 104. Iss. 7, p. 1005-1015. DOI: [10.2138/am-2019-6967](https://doi.org/10.2138/am-2019-6967)
9. Marschall H.R., Shao-Yong Jiang. Tourmaline Isotopes: No Element Left Behind. *Elements*. 2011. Vol. 7. N 5, p. 313-319. DOI: [10.2113/gselements.7.5.313](https://doi.org/10.2113/gselements.7.5.313)
10. van Hinsberg V.J., Franz G., Wood B.J. Determining subduction-zone fluid composition using a tourmaline mineral probe. *Geochemical Perspectives Letters*. 2017. Vol. 3. N 1, p. 160-169. DOI: [10.7185/geochemlet.1719](https://doi.org/10.7185/geochemlet.1719)
11. Trumbull R.B., Codeço M.S., Shao-Yong Jiang et al. Boron isotope variations in tourmaline from hydrothermal ore deposits: A review of controlling factors and insights for mineralizing systems. *Ore Geology Reviews*. 2020. Vol. 125. N 103682. DOI: [10.1016/j.oregeorev.2020.103682](https://doi.org/10.1016/j.oregeorev.2020.103682)
12. Da-Long Hu, Shao-Yong Jiang. In-situ elemental and boron isotopic variations of tourmaline from the Maogongdong deposit in the Dahutang W-Cu ore field of northern Jiangxi Province, South China: Insights into magmatic-hydrothermal evolution. *Ore Geology Reviews*. 2020. Vol. 122. N 103502. DOI: [10.1016/j.oregeorev.2020.103502](https://doi.org/10.1016/j.oregeorev.2020.103502)
13. Shimizu R., Ogasawara Y. Diversity of potassium-bearing tourmalines in diamondiferous Kokchetav UHP metamorphic rocks: A geochemical recorder from peak to retrograde metamorphic stages. *Journal of Asian Earth Sciences*. 2013. Vol. 63, p. 39-55. DOI: [10.1016/j.jseaes.2012.11.024](https://doi.org/10.1016/j.jseaes.2012.11.024)
14. Lussier A., Ball N.A., Hawthorne F.C. et al. Maruyamaite, $K(MgAl_2)(Al_5Mg)Si_6O_{18}(BO_3)_3(OH)_3O$, a potassium-dominant tourmaline from the ultrahigh-pressure Kokchetav massif, northern Kazakhstan: Description and crystal structure. *American Mineralogist*. 2016. Vol. 101. Iss. 2, p. 355-361. DOI: [10.2138/am-2016-5359](https://doi.org/10.2138/am-2016-5359)
15. Korsakov A.V., Travin A.V., Yudin D.S., Marshal H.R. $^{40}Ar/^{39}Ar$ dating of tourmaline from metamorphic rocks of the Kokchetav Massif, Kazakhstan. *Doklady Akademii nauk*. 2009. Vol. 424. N 4, p. 531-533 (in Russian).
16. Musiyachenko K.A., Korsakov A.V., Letnikov F.A. A new occurrence of maruyamaite. *Doklady Rossiiskoi Akademii nauk. Nauki o Zemle*. 2021. Vol. 498. N 1, p. 58-65 (in Russian). DOI: [10.31857/S268673972105011X](https://doi.org/10.31857/S268673972105011X)
17. Berryman E., Wunder B., Rhede D. Synthesis of K-dominant tourmaline. *American Mineralogist*. 2014. Vol. 99. N 2-3, p. 539-542. DOI: [10.2138/am.2014.4775](https://doi.org/10.2138/am.2014.4775)
18. Berryman E.J., Wunder B., Wirth R. et al. An experimental study on K and Na incorporation in dravitic tourmaline and insight into the origin of diamondiferous tourmaline from the Kokchetav Massif, Kazakhstan. *Contributions to Mineralogy and Petrology*. 2015. Vol. 169. Iss. 3. N 28. DOI: [10.1007/s00410-015-1116-9](https://doi.org/10.1007/s00410-015-1116-9)
19. Berryman E.J., Wunder B., Ertl A. et al. Influence of the X-site composition on tourmaline's crystal structure: investigation of synthetic K-dravite, dravite, oxy-uvite, and magnesio-foitite using SREF and Raman spectroscopy. *Physics and Chemistry of Minerals*. 2016. Vol. 43. N 2, p. 83-102. DOI: [10.1007/s00269-015-0776-3](https://doi.org/10.1007/s00269-015-0776-3)
20. Perchuk L.L., Safonov O.G., Yapaskurt V.O., Barton Jr J.M. Crystal-melt equilibria involving potassium-bearing clinopyroxene as indicator of mantle-derived ultrahigh-potassic liquids: an analytical review. *Lithos*. 2002. Vol. 60. Iss. 3-4, p. 89-111. DOI: [10.1016/S0024-4937\(01\)00072-X](https://doi.org/10.1016/S0024-4937(01)00072-X)
21. Safonov O.G., Perchuk L.L., Litvin Yu.A. Equilibrium K-Bearing Clinopyroxene-Melt as a Model for Barometry of Mantle-Derived Mineral Assemblages. *Russian Geology and Geophysics*. 2005. Vol. 46. N 12, p. 1318-1334 (in Russian).
22. Shatsky V.S., Skuzovatov S., Ragozin A.L., Sobolev N.V. Mobility of Elements in a Continental Subduction Zone: Evidence from the Uhp Metamorphic Complex of the Kokchetav Massif. *Russian Geology and Geophysics*. 2015. Vol. 56. N 7, p. 1016-1034.
23. Shyh-Lung Hwang, Pouyan Shen, Hao-Tsu Chu et al. Crust-derived potassic fluid in metamorphic microdiamond. *Earth and Planetary Science Letters*. 2005. Vol. 231. Iss. 3-4, p. 295-306. DOI: [10.1016/j.epsl.2005.01.002](https://doi.org/10.1016/j.epsl.2005.01.002)
24. Korsakov A.V., Hermann J. Silicate and carbonate melt inclusions associated with diamonds in deeply subducted carbonate rocks. *Earth and Planetary Science Letters*. 2006. Vol. 241. Iss. 1-2, p. 104-118. DOI: [10.1016/j.epsl.2005.10.037](https://doi.org/10.1016/j.epsl.2005.10.037)
25. Vasilev E.A., Kriulina G.Y., Garanin V.K. Thermal history of diamond from Arkhangelskaya and Karpinsky-I kimberlite pipes. *Journal of Mining Institute*. 2022. Vol. 255, p. 327-336. DOI: [10.31897/PMI.2022.57](https://doi.org/10.31897/PMI.2022.57)
26. Lavrova L.D., Pechnikov V.A., Pleshakov A.M. et al. New type of diamond deposits. Moscow: Nauchnyi mir, 1999, p. 221 (in Russian).
27. Sobolev N.V., Shatsky V.S. Diamond inclusions in garnets from metamorphic rocks: a new environment for diamond formation. *Nature*. 1990. Vol. 343. Iss. 6260, p. 742-746. DOI: [10.1038/343742a0](https://doi.org/10.1038/343742a0)
28. Dobretsov N.L., Sobolev N.V., Shatsky V.S. et al. Geotectonic evolution of diamondiferous paragneisses of the Kokchetav complex, Northern Kazakhstan – the geologic enigma of ultrahigh-pressure crustal rocks within Phanerozoic foldbelt. *The Island Arc*. 1995. Vol. 4. Iss. 4, p. 267-279. DOI: [10.1111/j.1440-1738.1995.tb00149.x](https://doi.org/10.1111/j.1440-1738.1995.tb00149.x)
29. Shatsky V.S., Sobolev N.V., Vavilov M.A. Diamond-bearing metamorphic rocks of the Kokchetav massif (northern Kazakhstan). *Ultra-High Pressure Metamorphism*. Cambridge: Cambridge University Press, 1995, p. 427-455.
30. Shatsky V.S., Ragozin A.L., Skuzovatov S.Yu. et al. Isotope-geochemical evidence of the nature of the protoliths of diamondiferous rocks of the Kokchetav subduction–collision zone (Northern Kazakhstan). *Geologiya i geofizika*. 2021. Vol. 62. N 5, p. 678-689 (in Russian). DOI: [10.15372/GiG2020200](https://doi.org/10.15372/GiG2020200)
31. Shatsky V.S., Skuzovatov S.Y., Ragozin A.L. Isotopic-Geochemical Evidence for Crustal Contamination of Eclogites in the Kokchetav Subduction-Collision Zone. *Russian Geology and Geophysics*. 2018. Vol. 59. N 12, p. 1560-1576 (in Russian) DOI: [10.15372/GiG20181203](https://doi.org/10.15372/GiG20181203).



32. Lavrentev Yu.G., Karmanov N.S., Usova L.V. Election Probe Microanalysis of Minerals: Microanalyser or Scanning Election Microscope? *Russian Geology and Geophysics*. 2015. Vol. 56. N 8, p. 1473-1482 (in Russian). DOI: [10.15372/GiG20150806](https://doi.org/10.15372/GiG20150806)
33. Le Zhang, Zhong-Yuan Ren, Nichols A.R.L. et al. Lead isotope analysis of melt inclusions by LA-MC-ICP-MS. *Journal of Analytical Atomic Spectrometry*. 2014. Vol. 29. Iss. 8, p. 1393-1405. DOI: [10.1039/C4JA00088A](https://doi.org/10.1039/C4JA00088A)
34. Whitney D.L., Evans B.W. Abbreviations for names of rock-forming minerals. *American Mineralogist*. 2010. Vol. 95. N 1, p. 185-187. DOI: [10.2138/am.2010.3371](https://doi.org/10.2138/am.2010.3371)
35. Henry D.J., Novák M., Hawthorne F.C. et al. Nomenclature of the tourmaline-supergrroup minerals. *American Mineralogist*. 2011. Vol. 96. N 5-6, p. 895-913. DOI: [10.2138/am.2011.3636](https://doi.org/10.2138/am.2011.3636)
36. Ota T., Kobayashi K., Kunihiro T., Nakamura E. Boron cycling by subducted lithosphere, insights from diamondiferous tourmaline from the Kokchetav ultrahigh-pressure metamorphic belt. *Geochimica et Cosmochimica Acta*. 2008. Vol. 72. Iss. 14, p. 3531-3541. DOI: [10.1016/j.gca.2008.05.002](https://doi.org/10.1016/j.gca.2008.05.002)
37. Ota T., Kobayashi K., Katsura T., Nakamura E. Tourmaline breakdown in a pelitic system: implications for boron cycling through subduction zones. *Contributions to Mineralogy and Petrology*. 2008. Vol. 155. Iss. 1, p. 19-32. DOI: [10.1007/s00410-007-0228-2](https://doi.org/10.1007/s00410-007-0228-2)
38. Celata B., Stagno V., Capizzi L.S. et al. Schorl breakdown at upper mantle conditions: Insights from an experimental study at 3.5 GPa. *Lithos*. 2022. Vol. 438-439. N 106999. DOI: [10.1016/j.lithos.2022.106999](https://doi.org/10.1016/j.lithos.2022.106999)
39. Ballirano P., Celata B., Bosi F. In situ high-temperature behaviour and breakdown conditions of uvite at room pressure. *Physics and Chemistry of Minerals*. 2022. Vol. 49. Iss. 10. N 40. DOI: [10.1007/s00269-022-01216-3](https://doi.org/10.1007/s00269-022-01216-3)
40. Hermann J., Spandler C.J. Sediment Melts at Sub-arc Depths: an Experimental Study. *Journal of Petrology*. 2008. Vol. 49. Iss. 4, p. 717-740. DOI: [10.1093/petrology/egm073](https://doi.org/10.1093/petrology/egm073)
41. Cheng L., Zhang C., Zhou Y. et al. Experiments reveal enrichment of ¹¹B in granitic melt resulting from tourmaline crystallization. *Geochemical Perspectives Letters*. 2022. Vol. 20, p. 37-42. DOI: [10.7185/geochemlet.2206](https://doi.org/10.7185/geochemlet.2206)
42. Selyatitskii A.Yu., Reverdatto V.V. Thermobaric Conditions for Exhumation of Ti-Clinohumite Garnetites of the Kokchetav Subduction-Collision Zone (Northern Kazakhstan). *Russian Geology and Geophysics*. 2022. Vol. 63. N 8, p. 1051-1074 (in Russian). DOI: [10.15372/GiG2021147](https://doi.org/10.15372/GiG2021147)
43. Xu J., Zhang G.B., Marschall H.R. et al. Boron isotopes of white mica and tourmaline in an ultra-high pressure metapelite from the western Tianshan, China: dehydration and metasomatism during exhumation of subducted ocean-floor sediments. *Contributions to Mineralogy and Petrology*. 2022. Vol. 177. Iss. 4. N 46. DOI: [10.1007/s00410-022-01916-7](https://doi.org/10.1007/s00410-022-01916-7)
44. Jan C.M. De Hoog, Savov I.P. Boron Isotopes as a Tracer of Subduction Zone Processes. *Boron Isotopes*. Cham: Springer International Publishing, 2018, p. 217-247. DOI: [10.1007/978-3-319-64666-4_9](https://doi.org/10.1007/978-3-319-64666-4_9)
45. Halama R., Konrad-Schmolke M., Jan C.M. De Hoog. Boron isotope record of peak metamorphic ultrahigh-pressure and retrograde fluid-rock interaction in white mica (Lago di Cignana, Western Alps). *Contributions to Mineralogy and Petrology*. 2020. Vol. 175. Iss. 3. N 20. DOI: [10.1007/s00410-020-1661-8](https://doi.org/10.1007/s00410-020-1661-8)
46. Stepanov A.S., Hermann J., Korsakov A.V., Rubatto D. Geochemistry of ultrahigh-pressure anatexis: fractionation of elements in the Kokchetav gneisses during melting at diamond-facies conditions. *Contributions to Mineralogy and Petrology*. 2014. Vol. 167. Iss. 5. N 1002. DOI: [10.1007/s00410-014-1002-x](https://doi.org/10.1007/s00410-014-1002-x)

Authors: Andrei V. Korsakov, Doctor of Geological and Mineralogical Sciences, Chief Researcher, korsakov@igm.nsc.ru, <https://orcid.org/0000-0002-4922-7658> (V.S.Sobolev Institute of Geology and Mineralogy Siberian Branch RAS, Novosibirsk, Russia), Denis S. Mikhailenko, Candidate of Geological and Mineralogical Sciences, Senior Researcher, <https://orcid.org/0000-0003-0585-3021> (V.S.Sobolev Institute of Geology and Mineralogy Siberian Branch RAS, Novosibirsk, Russia), Le Zhang, PhD, Head of Laboratory, <https://orcid.org/0000-0001-9161-0653> (State Key Laboratory of Isotope Geochemistry and CAS Center for Excellence in Deep Earth Science, Guangzhou Institute of Geochemistry, Chinese Academy of Science, Guangzhou, China), Yi-Gang Xu, Academician Chinese of Science, Professor, <https://orcid.org/0000-0002-9531-7208> (State Key Laboratory of Isotope Geochemistry and CAS Center for Excellence in Deep Earth Science, Guangzhou Institute of Geochemistry, Chinese Academy of Science, Guangzhou, China).

The authors declare no conflict of interests.